Journal of Chemical and Petroleum Engineering 2020, 54(1): 1-12
DOI: 10.22059/jchpe.2020.254905.1225

RESEARCH PAPER

Optimization of Extended UNIQUAC Model Parameter for Mean Activity Coefficient of Aqueous Chloride Solutions using Genetic+PSO

Seyed Hossein Hashemi[a], Mahmood Dinmohammad[b,*], Mehrdad Bagheri[c]

a. Department of Chemical Engineering, University of Mohaghegh Ardabili, Ardabil, Iran
b. Institute of Production and Recovery, Research Institute of Petroleum Industry, Tehran, Iran
c. Petroleum University of Technology, Ahwaz, Iran

Received: 2 April 2018, Revised: 19 December 2019, Accepted: 14 March 2020

Abstract

In the present study, in order to predict the activity coefficient of inorganic ions, 12 cases of aqueous chloride solution were considered (AClx=1,2; A=Li, Na, K, Rb, Mg, Ca, Ba, Mn, Fe, Co, Ni). For this study, the UNIQUAC thermodynamic model is desired and its adjustable parameters are optimized with the genetic+particle swarm optimization (PSO) algorithm. The optimization of the UNIQUAC model with PSO+genetic algorithms has good results. So that the minimum and maximum electrolyte error of the whole system are 0.00044 and 0.0091, respectively. For this study, a temperature of 298.15 and a pressure of 1 is considered. Also, in this study for the electrolyte system, the Artificial bee colony (ABC) algorithm, and Imperialist competitive algorithm (ICA) has been studied. The results showed that the Artificial bee colony algorithm has a lower accuracy than the genetic + PSO algorithm. The minimum concentration was 0.1 Molality and the maximum concentration was 3 Molality. Based on the results, the activity coefficient of LiCl, NaCl, KCl, RbCl + H_2O, $MgCl_2$, $CaCl_2$, $BaCl_2$, $MnCl_2$, $FeCl_2$, $CoCl_2$ $NiCl_2$ depends on the ionic strength of the electrolyte system.

Keywords:
Artificial Bee Colony Algorithm,
Extended UNIQUAC Model,
Genetic+PSO Algorithm,
Mineral Ions,
Optimization

Introduction

Nowadays, due to presence of electrolyte solutions in most of the chemical processes in the industry [1-5], it is very important to investigate the nature of the chemical behavior and the phase of liquids during the process (Such as control of electrolyte concentration in end products during effluent flow). Electrolyte solutions cover a wide range of compounds (aqueous, organic, and dilute) and specific conditions (from ambient temperature to supercritical conditions) [6,7]. Therefore, predicting the thermodynamic properties of electrolyte solutions seems necessary and important. The study of the thermodynamic properties of electrolyte systems (such as ion activity coefficient, water activity, osmotic coefficient, and ion solubility) has been studied by researchers.

Hashemi [8] investigated the solubility of barium sulfate at temperatures and pressures in a thermodynamic study. According to the results of his study, the solubility of barium sulfate decreased with increasing temperature. Also, with increasing pressure (from 10 to 1000 bar), the solubility of barium sulfate is increased. In Hashemi's research, water activity was studied in the equilibrium system of manganese sulfate + water and nickel sulfate + water (at different temperatures and pressures). Hashemi et al. [9] investigated the activity coefficient of inorganic

* Corresponding author:
Email: dinmohammadm@ripi.ir (M. Dinmohammad)

ions for a multicomponent system. In their study barium, calcium, strontium, chlorine, carbonate, sulfate, and other ions were considered. In their study, the solubility of barium sulfate, strontium in the presence of sodium chloride, calcium chloride, and magnesium chloride were predicted. In a study, Hashemi et al. [10] Optimized the EUNIQUAC model based on experimental results to predict water activity in electrolyte systems (based on chloride and sulfate solution). In their study, water activity for equilibrium systems such as AClx = 1,2; A = Li, H, Na, K, NH_4, Cs, Mg, Ca, Ba and Bj = 1,2SO_4; B = Li, Na, K , NH_4, Mg, Mn, Ni, Cu, Zn, and NaCl + $LaCl_3$ (aq), NaCl + $MgCl_2$ (aq), Na_2SO_4 + $MgSO_4$ (aq) was studied. In a research work to investigate mineral deposition in petroleum systems, Hashemi et al. [11] Investigated the solubility of calcium sulfate in the presence of magnesium chloride and calcium chloride under different temperature conditions. According to the results of their study, the solubility of calcium sulfate increases with increasing temperature due to magnesium chloride and calcium chloride concentrations. Alhajri et al. [12] Investigated the solubility of $BaSO_4$ in single salt solutions containing NaCl, $CaCl_2$, $MgCl_2$, KCl, KBr, Na_2SO_4 and Na_2B4O_7 and the solubility of $SrSO_4$ in single, binary and trivalent salt solutions containing NaCl, $CaCl_2$, and $MgCl_2$.

Due to the thermodynamic force between ions, electrolyte solutions are one of the most important aquatic systems in the chemical industry (prediction of mineral deposition in oilfields). Therefore, in the present study, the optimization of the parameters of the UNIQUAC model (using optimization algorithms) is studied to investigate the effect of ion concentration on the activity coefficients of inorganic ions in the electrolyte system.

In this research, EUNIQUAC model due to ion activity coefficient for electrolytic systems (LiCl + H_2O, NaCl + H2O, KCl + H_2O, RbCl + H_2O, $MgCl_2$ + H_2O, $CaCl_2$ + H_2O, $BaCl_2$ + H_2O, $FeCl_2$ + H_2O, $MnCl_2$ + H_2O + and $NiCl_2$ + H_2O have been investigated by genetic optimization+particle optimization (PSO), Artificial Bee Colony (ABC) and Imperialist Competitive Algorithm (ICA). Simulation of polymer flooding with low salinity has been performed on the core scale using a commercial reservoir simulator (Eclipse 100). Four scenarios have been designed to investigate the effect of salinity on the simulation of polymer flooding. Due to the lack of experimental relative permeability data, in order to accurately simulate core-scale polymer flooding, the simulator has been coupled with MATLAB software to generate relative permeability and capillary pressure curves using automatic history matching. Different optimization algorithms and relative permeability correlations have been used to obtain the best match with the experimental data. In the last section of this study, the results of simulation of low salinity polymer flooding in a long core model are presented.

The Model and Solution Method

The Extended UNIQUAC Activity Coefficient Equation

In this work, model Extended UNIQUAC (as presented by Thomsen and Rasmussen [13]) is desired to study the electrolytic system, that temperature and concentration parameters of the study variables. This model is a combination of the UNIQUAC model and the Debye-Hückel term. This method, is less than the required number of parameters, compared to similar models, such as the Pitzer model. The UNIQUAC model presented by Abrams and Prausnitz [14] for excess Gibbs free energy of a mixture and consists of two parts: the first part is combinatorial that is related to the entropy of the system and has been determined based on the size and shape of the molecules. The residual part is related to intermolecular forces involved in the enthalpy of mixing and depends on the intermolecular forces. The UNIQUAC equation has adjustable parameters, which are expressed as follows for a liquid-solid (or liquid-vapor) equilibrium in the binary and multicomponent system [15-16]:

$$G^{\mathrm{E}} = G^{E}{}_{combinatorial} + G^{E}{}_{Residual} + G^{E}{}_{Debye-HucKel} \quad (1)$$

$$\frac{G^{E}{}_{combinatorial}}{\mathrm{RT}} = \sum x_i \, ln \left(\frac{\emptyset_i}{x_i}\right) - \frac{\mathrm{Z}}{2} \sum q_i x_i \, ln \left(\frac{\emptyset_i}{\theta_i}\right) \quad (2)$$

In the above equation, G^E is Gibbs free energy. In Eq. 2, z is coordination number and its value is equal to 10; x_i is mole fraction; ϕ_i is volume fraction and θ_i is the surface area fraction of ions in the liquid-solid or liquid-vapor equilibrium system which is expressed as:

$$\emptyset_{\mathrm{i}} = \frac{\mathrm{x_i r_i}}{\sum_{\mathrm{l}} \mathrm{x_l r_l}} \quad (3)$$

$$\theta_{\mathrm{i}} = \frac{\mathrm{x_i q_i}}{\sum_{\mathrm{l}} \mathrm{x_l q_l}} \quad (4)$$

where r_i and q_i are the volume and surface area parameters for each ion. Also, for the residual term, the following equation holds:

$$\frac{G^{E}{}_{Residual}}{RT} = -\sum_{i} q_i x_i \, ln \left(\sum_{k} \theta_{\mathrm{k}} \varphi_{ki}\right) \quad (5)$$

$$\varphi_{ij} = \exp\left(-\frac{u_{ij} - u_{ii}}{T}\right) \quad (6)$$

u_{ii} is energy interaction between similar ions in an equilibrium system of solid-liquid and vapor-liquid. u_{ij} is energy interaction between different ions in an equilibrium system with each other. The energy interaction is a function of temperature and is defined as:

$$u_{ij} = u_{ij}{}^{\circ} + u_{ij}{}^{t} \, (T - 298.15) \quad (7)$$

$u_{ij}{}^{0}$ and $u_{ij}{}^{t}$ are two adjustable parameters for energy interaction between the ions in the equilibrium system.

The Debye-Hückel contribution (to the excess Gibbs energy) of the extended UNIQUAC model is given by the expression:

$$\frac{G^{E}{}_{Debye-HucKel}}{RT} = -x_w M_w \frac{4A}{b^3} \left[\ln\left(1 + bI^{\frac{1}{2}}\right) - bI^{\frac{1}{2}} + \frac{b^2 I}{2}\right] \quad (8)$$

where M_w is the molar mass of water, x_w is the mole fraction of water, A is a Debye-Hückel parameter, b is a constant equal to 1.5 $(kg/mol)^{0.5}$ and I is the ionic strength.

$$A = a_0 + a_1(T - 273.15) + a_2 (T - 273.15)^2 \quad (9)$$

$$\mathrm{I} = 0.5 \sum \mathrm{m_i Z_i}^2 \quad (10)$$

In this equation, z_i and m_i are is the charge and the molality (mol/(kg H_2O)$^{-1}$) of ion i. Finally, we will have:

$$\begin{aligned} \ln \gamma_i{}^{*} = {} & \ln\left(\frac{\emptyset_i}{x_i}\right) + 1 - \frac{\emptyset_i}{x_i} - \frac{z}{2}.q_i \left[\ln\left(\frac{\emptyset_i}{\theta_i}\right) + 1 - \frac{\emptyset_i}{\theta_i}\right] - ln\left(\frac{r_i}{r_w}\right) + 1 - \frac{r_i}{r_w} \\ & - \frac{z}{2}.q_i \left[\ln\left(\frac{\mathrm{r_i}.\mathrm{q_w}}{\mathrm{r_w q_i}}\right) + 1 - \frac{\mathrm{r_i}.\mathrm{q_w}}{\mathrm{r_w q_i}}\right] + q_{\mathrm{i}} \left[1 - \ln\left(\sum_{\mathrm{k}} \theta_{\mathrm{k}} \varphi_{\mathrm{lk}}\right) - \sum_{\mathrm{k}} \frac{\theta_{\mathrm{k}} \varphi_{\mathrm{ik}}}{\sum \theta_{\mathrm{l}} \varphi_{\mathrm{lk}}}\right] \\ & - \mathrm{q_i}[1 - \ln(\varphi_{\mathrm{wi}}) - \varphi_{\mathrm{iw}}] - Z_i{}^2 \frac{AI^{1/2}}{1 + bI^{1/2}} \end{aligned} \quad (12)$$

Solution Method

The flowchart optimization EUNIQUAC model, shown by genetic+particle swarm optimization algorithms (PSO), Artificial bee colony (ABC) Algorithms and Imperialist competitive Algorithms (ICA) to determine the average activity coefficient in Fig. 1. As shown in Fig. 1, the temperature and initial concentration (based on molality units) loaded to the model. The variables of u^{o} ،u^{t} ،q and r are considered as adjustable variables for optimization. Since the activity coefficient model of Extended UNIQUAC is calculated based on molar ratios, the initial concentration should be unit-converted from molality to molar ratio. According to the criteria defined error and the objective function if error acceptability, the optimization process stops and the results will be printed. The computation process will go on until the error criterion is met. In the appendix, the MATLAB code for the EUNIQUAC model is shown.

Optimization Algorithms in This Research

Hybrid Genetic Algorithm-Particle Swarm Algorithm

This algorithm is based on a dynamic method that combines two advanced genetic search algorithms and the PSO algorithm. The genetic algorithm is sensitive to the initial population in the process of searching for the optimal value, which is related to the random nature of the operators of the genetic optimization algorithm. This can cause a deviation in the optimization process of the objective function. In other words, due to the considerable dependence of the genetic algorithm on the initial population, the genetic algorithm may never converge if the optimal primary population is not selected. One of the special features of the PSO algorithm is the fast convergence toward the optimal value at the beginning of the search and slow convergence process near the optimal value. So, combining these two algorithms can solve the problems in the computational process [17-18].

Imperialist Competitive Algorithm

The imperialist competitive algorithm is a method in the field of evolutionary computation. The colonial competition algorithm also constitutes an initial set of possible solutions (country). This algorithm gradually improves the initial solutions (countries) and finally provides the appropriate solution to the optimization problem (desirable country). We choose the best members of this population (the countries with the least cost function) as imperialists. With the formation of the early empires, colonial competition between them began and any empire that failed to succeed in the colonial competition would be eliminated from the scene of colonial competition. As a result, in the process of colonial rivalries (gradually increasing the power of the larger empires), the weaker empires disappear [19].

Artificial Bee Colony Algorithm

The artificial bee colony algorithm (ABC) is an optimization algorithm based on the intelligent behavior of the bee population. Artificial bee colony algorithm (ABC) consists of three groups of employed bees (honeybees that go to predetermined food sources), onlookers (bees that remain in the area of choice for a food source), and scouts (This bee is responsible for finding new food, new nectar, and resources). In the ABC algorithm, the position of a food source represents an optimization solution and the nectar value of the food source is related to the suitability of the solution [20-22].

Results and Discussion

In this research, the described flowchart has brought very good results after running the application for LiCl+H_2O, NaCl+H_2O, KCl+H_2O, RbCl+H_2O, $MgCl_2$+H_2O, CaCl2+H_2O, $BaCl_2$+H_2O, $MnCl_2$+H_2O, $FeCl_2$+H_2O, $CoCl_2$+H_2O and $NiCl_2$+H_2O, and Temperature changes 298.15 k; that the total error based on error equation in Table 1 is reported. Optimization results (using three algorithms) are shown in Table 1. According to this table, the error rate of the objective function of the hybrid optimization algorithm for the NaCl system is 0.000925. The results of ICA and ABC algorithms were 0.038 and 0.365, respectively. The results of Table 1 indicate the desired accuracy of the genetic+PSO algorithm over the other two algorithms (ABC and ICA).

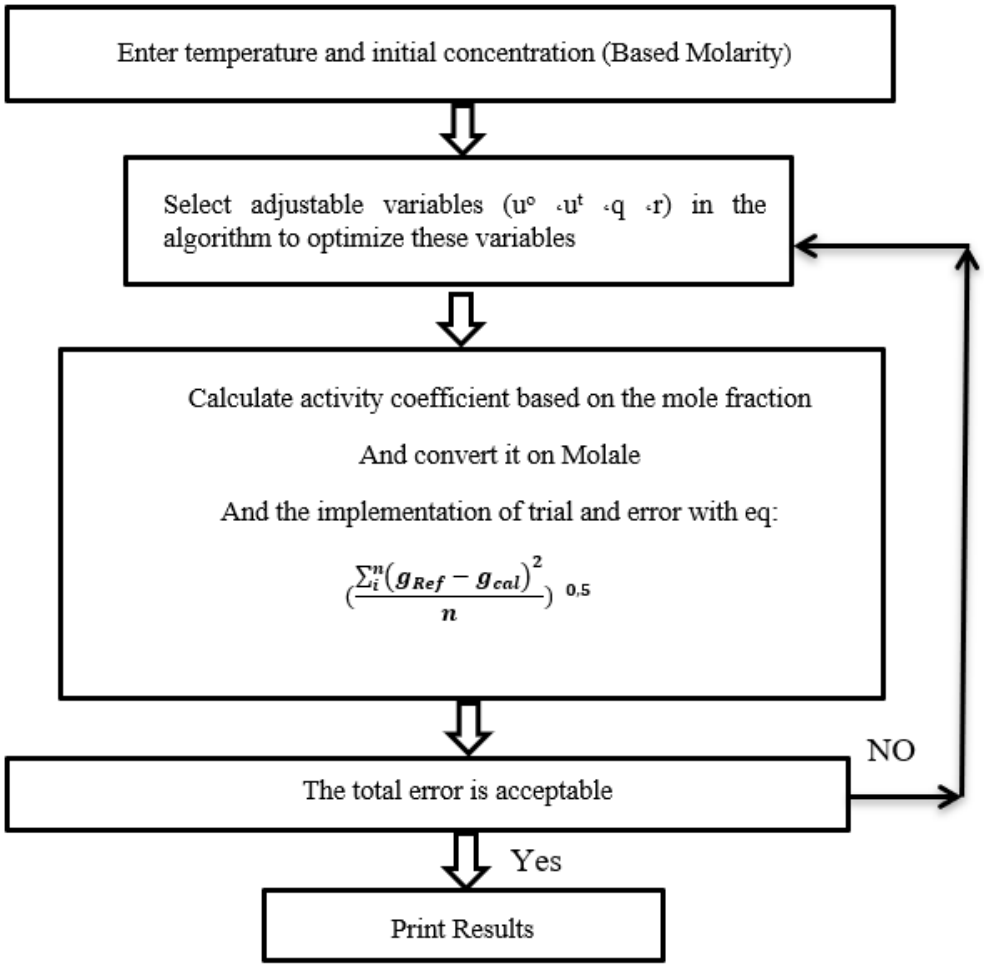

Fig. 1. The process of optimizing the average activity coefficient model based on genetic algorithm

The parameter u, r, and q are considered as 3 adjustable variables in the theoretical model of this study. These 3 parameters were considered as adjustable and constant variables during the optimization process. U parameter is more important than the other two parameters due to its dependence on the energy interaction between the ions. In total, 17 variables in the algorithm were considered for optimization. In other words, given the appropriate activity coefficient (based on the objective function), these 17 parameters will reach ideal constant values. In the flowchart optimization algorithm for these parameters was considered two upper and lower limits.

Table1. Total error based on defined error equation for electrolyte solutions using genetic+PSO, ABC algorithms and Imperialist competitive algorithm (ICA)

Electrolyte Solutions	Total error with genetic+PSO	Total error with ABC	Total error with ICA
$LiCl+H_2O$	0.000717	0.122	0.047
$NaCl+H_2O$	0.000925	0.365	0.038
$KCl+H_2O$	0.0024	0.267	0.033
$RbCl+H_2O$	0.0014	0.25	0.073
$MgCl_2+H_2O$	0.0052	0.247	0.042
$CaCl_2+H_2O$	0.0081	0.28	0.01
$BaCl_2+H_2O$	0.0031	0.19	0.027
$MnCl_2+H_2O$	0.00044	0.205	0.058
$FeCl_2+H_2O$	0.0091	0.3006	0.14
$CoCl_2+H_2O$	0.003	0.23	0.085
$NiCl_2+H2O$	0.0019	0.25	0.068
$SrCl_2+H_2O$	0.0029	0.21	0.058

Fig. 2, shows the optimization of the mean activity coefficient of the electrolyte solution at constant pressure 1 bar and Temperatures 298.15 K using the EUNIQUAC model and genetic+PSO algorithm. According to Fig. 2, in the concentration of 1 molality, the highest and lowest average activity coefficient, sodium chloride, and barium chloride is dedicated. Also, according to the results of Fig. 2, with increasing concentration of the aqueous solution from 0 to 1.5 molality, the process of average activity coefficient for calcium chloride, iron chloride, magnesium chloride, strontium chloride, manganese chloride, and nickel chloride has been associated with an increase. However, with increasing concentration of the aqueous solution from 0 to 1.5 molality, the process of average activity coefficient for NaCl, RbCl, KCl, and Bacl2 declined.

In Figs. 3 and 4, is shown, the average activity coefficient of $CoCl_2$ and $NiCl_2$ at various concentrations in the electrolytic system according to the genetic+PSO algorithm. According to the results of Figs. 3 and 4, the coefficient of activity of $CoCl_2$ and $NiCl_2$ decreases with increasing concentration of $CoCl_2$ and $NiCl_2$ in the interval (0.1 to 0.5 mol). However, from the interval of 0.5 to 1.4 molality, the trend of $CoCl_2$ and $NiCl_2$ activity coefficient is increasing. Based on the results of Figs. 2 to 4, the activity coefficient of LiCl, NaCl, KCl, RbCl + H_2O, $MgCl_2$, $CaCl_2$, $BaCl_2$, $MnCl_2$, $FeCl_2$, $CoCl_2$, and $NiCl_2$ depends on the ionic strength of the electrolyte system.

Table 2 compares, the average activity coefficient predictions of electrolyte systems at the constant pressure of 1 bar and temperatures of 298.15 K using the theoretically optimized model in this research to experimental results. Comparing the results demonstrated in Table 2 emphasizes that the optimized model in this research (Similar to the thermodynamic model in [23]) is significantly acceptable.

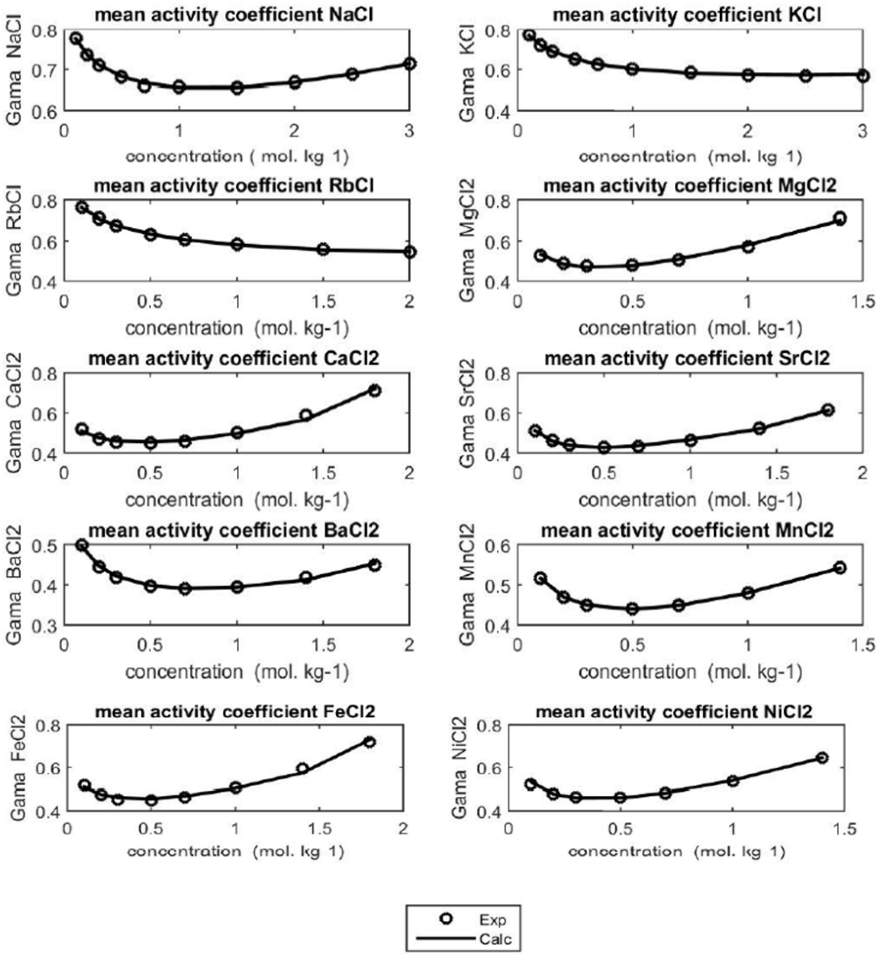

Fig. 2. Comparison between the mean activity coefficient values predicted by the model and experimental data (Experimental [23])

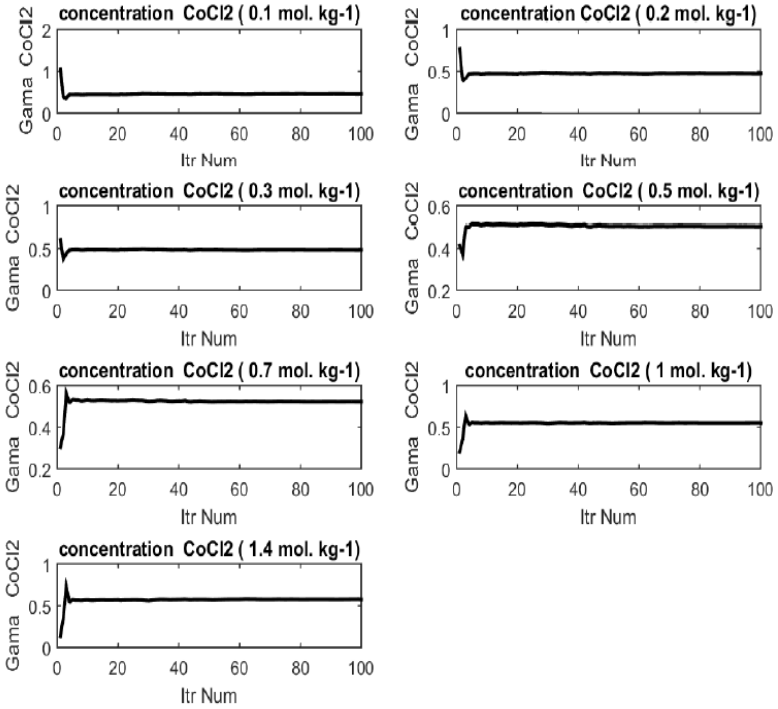

Fig. 3. The process of the activity coefficient of $CoCl_2$ at various concentrations by genetic+PSO Algorithm

Table 2. Comparison between activity coefficient values predicted by the model and experimental data at molalities of aqueous chloride solutions

m	Exp [23]	Calc This Work	Calc [23]	m	Exp [23]	Calc This Work	Calc [23]	m	Exp [23]	Calc This Work	Calc [23]
		NaCl				KCl				RbCl	
0.1	0.778	0.776	0.776	0.1	0.77	0.768	0.767	0.1	0.764	0.761	0.762
0.2	0.735	0.735	0.731	0.2	0.718	0.719	0.716	0.2	0.709	0.71	0.708
0.3	0.71	0.711	0.707	0.3	0.688	0.689	0.686	0.3	0.675	0.677	0.676
0.5	0.681	0.682	0.679	0.5	0.649	0.649	0.649	0.5	0.634	0.634	0.635
0.7	0.667	0.666	0.66	0.7	0.626	0.625	0.626	0.7	0.608	0.607	0.609
1	0.657	0.655	0.657	1	0.604	0.601	0.606	1	0.583	0.580	0.584
1.5	0.656	0.6557	0.659	1.5	0.583	0.582	0.586	1.5	0.559	0.557	0.558
2	0.668	0.668	0.671	2	0.573	0.573	0.576	2	0.546	0.5475	0.542
2.5	0.688	0.6884	0.691	2.5	0.569	0.572	0.571				
3	0.714	0.713	0.716	3	0.569	0.574	0.571				
		$MgCl_2$				$CaCl_2$				$SrCl_2$	
0.1	0.529	0.533	0.53	0.1	0.518	0.509	0.519	0.1	0.511	0.513	0.511
0.2	0.489	0.484	0.489	0.2	0.472	0.475	0.472	0.2	0.462	0.460	0.461
0.3	0.477	0.470	0.477	0.3	0.455	0.460	0.454	0.3	0.442	0.438	0.441
0.5	0.481	0.478	0.481	0.5	0.448	0.454	0.448	0.5	0.43	0.427	0.43
0.7	0.506	0.510	0.506	0.7	0.46	0.464	0.46	0.7	0.434	0.437	0.436
1	0.57	0.581	0.572	1	0.5	0.498	0.499	1	0.461	0.467	0.462
1.4	0.709	0.702	0.714	1.4	0.587	0.567	0.586	1.4	0.524	0.521	0.524
				1.8	0.712	0.7209	0.72	1.8	0.614	0.613	0.619
		$BaCl_2$				$MnCl_2$				$FeCl_2$	
0.1	0.5	0.496	0.496	0.1	0.516	0.516	0.514	0.1	0.518	0.508	0.518
0.2	0.444	0.447	0.44	0.2	0.469	0.469	0.466	0.2	0.473	0.476	0.472
0.3	0.419	0.421	0.415	0.3	0.45	0.449	0.446	0.3	0.454	0.462	0.454
0.5	0.397	0.397	0.393	0.5	0.44	0.439	0.438	0.5	0.45	0.457	0.449
0.7	0.391	0.390	0.388	0.7	0.448	0.448	0.447	0.7	0.463	0.468	0.462
1	0.395	0.394	0.395	1	0.479	0.479	0.479	1	0.506	0.503	0.504
1.4	0.419	0.412	0.42	1.4	0.542	0.541	0.55	1.4	0.596	0.574	0.594
1.8	0.449	0.453	0.458					1.8	0.719	0.729	0.731
		CoCl2				NiCl2					
0.1	0.522	0.518	0.523	0.1	0.522	0.523	0.523				
0.2	0.479	0.477	0.479	0.2	0.479	0.477	0.479				
0.3	0.463	0.462	0.464	0.3	0.463	0.461	0.464				
0.5	0.462	0.464	0.463	0.5	0.464	0.461	0.463				
0.7	0.479	0.485	0.481	0.7	0.482	0.483	0.482				
1	0.531	0.537	0.533	1	0.536	0.54	0.535				
1.4	0.634	0.627	0.644	1.4	0.647	0.644	0.65				

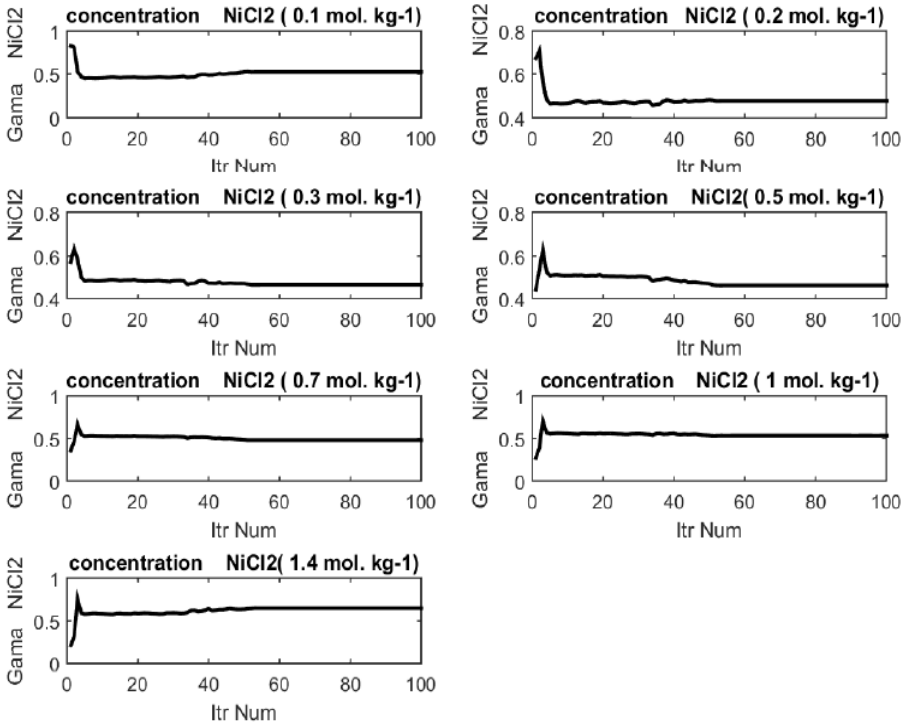

Fig4. The process of the activity coefficient of $NiCl_2$ at various concentrations by genetic+PSO Algorithm

Conclusions

In this study, in order to predict the activity coefficient of inorganic ions, 12 aqueous chloride solutions were investigated. For this study, the adjustable parameters of the EUNIQUAC model were optimized with the PSO+genetic algorithm. Based on the results, the hybrid algorithm has better accuracy and response in the optimization process. The optimal error rate for the lithium chloride aqueous solution is 0.000717 and based on the ABC algorithm and ICA algorithm are 0.122 and 0.047, respectively. According to the results, the coefficient of activity of $CoCl_2$ and $NiCl_2$ decreases with increasing concentration of $CoCl_2$ and $NiCl_2$ in the interval (0.1 to 0.5 mol). However, from the interval of 0.5 to 1.4 molality, the trend of $CoCl_2$ and $NiCl_2$ activity coefficient is increasing. Based on the results of Figs. 2 to 4, the activity coefficient of LiCl, NaCl, KCl, RbCl + H_2O, $MgCl_2$, $CaCl_2$, $BaCl_2$, $MnCl_2$, $FeCl_2$, $CoCl_2$, and $NiCl_2$ depends on the ionic strength of the electrolyte system.

Appendix

```
function Cost = CostFunc (X)
for ii = 1:size(X)
   r(1,1) = X(ii,1);
   r(1,2) = X(ii,2);
   r(1,3) = X(ii,3);
   q(1,1) = X(ii,4);
   q(1,2) = X(ii,5);
   q(1,3) = X(ii,6);
   a = X(ii,7);
   b = X(ii,8);
   c = X(ii,9);
    t=X(ii,10);
   e = X(ii,11);
```

```
    d = X(ii,12);
    h = X(ii,13);
    f=X(ii,14);
   p0=X(ii,15);
   p1=X(ii,16);
   p2=X(ii,17);
format long
u0=[0   a    b
       a   0    c
        b   c   t ];
ut=[0   e   d
      e   0   h
       d   h   f ];
  %%%%%%%%%%
 z=[zwarer  zcatons   zanions];
     T  = 298.15  %  T= Kelvin
    Rag=8.314;
    x=[xwater   xcatons   xanions];
    xq=x.*q;
    xr=x.*r;
    theta=xq/sum(xq);
    fi=xr/sum(xr);
    u= u0+ ut.*(T-298.15);
   v=x(1).*0.018;
   I=0.5.*(sum(x.*z)/(v));
     L=p0+(p1*(T-273))+(p2*(T-273.15)^2);
    w=(z.^0.5).*((L.*I.^0.5)/1+1.5.*I.^0.5);
    for i=1:3
       for j=1:3
          psi(i,j)=exp (-(u(i,j)-u(j,j))./(Rag.*T));
       end
    end
    for i=1:3
       for j=1:3
          n=(theta*psi);
          a(j,i)= (theta(1,j).*psi(i,j));
          A(i,j)=a(j,i)./n(i);
          C= sum(A');
          s=theta*psi;
       end
    end
    for i=1:3
       for  j= 1:3
          gama2(1,j)= log(fi(1,j)/x(1,j)) +1- (fi(1,j)/x(1,j)) -5*q(1,j)*(log(fi(1,j)/theta(1,j))+1-
(fi(1,j)/theta(1,j)))-(log (r(1,j)/r(1))+1 -(r(1,j)/r(1))-5*q(1,j)*(log ((r(1,j)*q(1))/(r(1)*q(1,j)))+
1-((r(1,j)*q(1))/(r(1)*q(1,j)))));
          gama1(1,j)=q(1,j).*(1-log(s(1,j))-(C(1,j)))-q(1,j).*(1-log(psi(1,j))-psi(j,1));
       end
    end
    gama1f = exp(gama1+gama2-w)*xwater
```

```
    gn= (gama1f(2)*gama1f(3)).^0.5;  % n=1,2,….
%%%%
 G=[g1  g2  g3  …… gn] ;
E=[e1  e2   e3   ..... en ];
Cost(ii,1) = ((1/N).*sum((G -E).^2)).^0.5  ; %  N=1 ,2 ,3 ,….,n
```

References

[1] Hashemi SH, Hashemi SA. Prediction of scale formation according to water injection operations in Nosrat Oil Field. Modeling Earth Systems and Environment. 2020 Mar;6(1):585-9.

[2] Hashemi SH, Mousavi Dehghani SA, Dinmohammad M. Thermodynamic Prediction of Ba and Sr Sulfates Scale Formation in Waterflooding Projects in Oil Reservoirs. Journal of Mineral Resources Engineering. 22;4(2):23-37.

[3] Otumudia E, Awajiogak U. Determining the Rates for Scale Formation in Oil Wells, International Journal of Engineering Research and Applications. 2016;6(9 Part 1):62-6.

[4] Haghtalab A, Kamali MJ, Shahrabadi A. Prediction mineral scale formation in oil reservoirs during water injection. Fluid Phase Equilibria. 2014 Jul 15;373:43-54.

[5] El-Said M, Ramzi M, Abdel-Moghny T. Analysis of oilfield waters by ion chromatography to determine the composition of scale deposition. Desalination. 2009 Dec 15;249(2):748-56.

[6] Bromley LA. Thermodynamic properties of strong electrolytes in aqueous solutions. AIChE Journal. 1973 Mar;19(2):313-20.

[7] Chen CC, Evans LB. A local composition model for the excess Gibbs energy of aqueous electrolyte systems. AIChE Journal. 1986 Mar;32(3):444-54.

[8] Hashemi SH. Thermodynamic study of water activity of single strong electrolytes. Journal of Applied and Computational Mechanics. 2017 Jun 1;3(2):150-7.

[9] Hashemi SH, Dehghani SA, Khodadadi A, Dinmohammad M, Hosseini SM, Hashemi SA. Optimization of Extended UNIQUAC Parameter for Activity Coefficients of Ions of an Electrolyte System using Genetic Algorithms. Korean Chemical Engineering Research. 2017;55(5):652-9.

[10] Hashemi SH, Dehghani SA, Dinmohammad M, Hashemi SA. Prediction of Water Activity of Electrolyte Solutions with Extended UNIQUAC Model. Journal of Chemical and Pharmaceutical Research. 2017;9(1):247-52.

[11] Hashemi SH, Mousavi Dehghani SA, Dinmohammad M, Hashemi SA. Thermodynamic prediction of anhydrite mineral deposit formation in petroleum electrolytic solutions. Nashrieh Shimi va Mohandesi Shimi Iran (NSMSI) 2018 July 4.

[12] Alhajri IH, Alarifi IM, Asadi A, Nguyen HM, Moayedi H. A general model for prediction of $BaSO_4$ and SrSO4 solubility in aqueous electrolyte solutions over a wide range of temperatures and pressures. Journal of Molecular Liquids. 2020 Feb 1;299:112142.

[13] Thomsen K, Rasmussen P. Modeling of vapor–liquid–solid equilibrium in gas–aqueous electrolyte systems. Chemical Engineering Science. 1999 Jun 1;54(12):1787-802.

[14] Abrams DS, Prausnitz JM. Statistical thermodynamics of liquid mixtures: a new expression for the excess Gibbs energy of partly or completely miscible systems. AIChE Journal. 1975 Jan;21(1):116-28.

[15] Sander B, Rasmussen P, Fredenslund A. Calculation of solid-liquid equilibria in aqueous solutions of nitrate salts using an extended UNIQUAC equation. Chemical Engineering Science. 1986 Jan 1;41(5):1197-202.

[16] García AV, Thomsen K, Stenby EH. Prediction of mineral scale formation in geothermal and oilfield operations using the extended UNIQUAC model: part I. Sulfate scaling minerals. Geothermics. 2005 Feb 1;34(1):61-97.

[17] Langeveld J, Engelbrecht AP. A generic set-based particle swarm optimization algorithm. InInternational conference on swarm intelligence, ICSI. 2011 Jun (pp. 1-10).

[18] Murthy KR, Raju MR, Rao GG. Comparison between conventional, GA and PSO with respect to optimal capacitor placement in agricultural distribution system. In2010 Annual IEEE India Conference (INDICON) 2010 Dec 17 (pp. 1-4). IEEE.

[19] Ghasemi M, Ghavidel S, Rahmani S, Roosta A, Falah H. A novel hybrid algorithm of imperialist competitive algorithm and teaching learning algorithm for optimal power flow problem with non-smooth cost functions. Engineering Applications of Artificial Intelligence. 2014 Mar 1;29:54-69.
[20] Basturk B. An artificial bee colony (ABC) algorithm for numeric function optimization. InIEEE Swarm Intelligence Symposium, Indianapolis, IN, USA, 2006.
[21] Karaboga D, Basturk B. A powerful and efficient algorithm for numerical function optimization: artificial bee colony (ABC) algorithm. Journal of global optimization. 2007 Nov 1;39(3):459-71.
[22] Karaboga D, Basturk B. On the performance of artificial bee colony (ABC) algorithm. Applied Soft Computing. 2008 Jan 1;8(1):687-97.
[23] Stokes RH, Robinson RA. Ionic hydration and activity in electrolyte solutions. Journal of the American Chemical Society. 1948 May;70(5):1870-8.